OXFORD JLB JOURNAL OF LEUKOCYTE BIOLOGY

Journal of Leukocyte Biology, 2025, **117**, qiae178

https://doi.org/10.1093/jleuko/qiae178
Advance access publication 23 August 2024
Article

Leukemia inhibitory factor drives transcriptional programs that promote lipid accumulation and M2 polarization in macrophages

Visnu Chaparro,[1,*] Louis-Philippe Leroux,[1] Aurore Lebourg,[1] Sophie Chagneau,[1] Tyson E. Graber,[2] Tommy Alain,[2,3] and Maritza Jaramillo[1,*]

[1]Institut National de la Recherche Scientifique (INRS) - Centre Armand-Frappier Santé Biotechnologie (CAFSB), 531 boul. des Prairies, Laval, QC H7V 1B7, Canada
[2]Children's Hospital of Eastern Ontario Research Institute, 401 Smith Rd. Ottawa, ON K1H 8L1, Canada
[3]Department of Biochemistry, Microbiology and Immunology, 75 Laurier Ave E. University of Ottawa, Ottawa, ON K1N 6N5, Canada
*Corresponding authors: INRS - CAFSB, 531 boul. des Prairies, Laval, QC H7V 1B7, Canada. Email: maritza.jaramillo@inrs.ca (M.J.); or visnu.chaparro@inrs.ca (V.C.)

Abstract

Leukemia inhibitory factor, a member of the interleukin-6 cytokine family, plays a central role in homeostasis and disease. Interestingly, some of the pleiotropic effects of leukemia inhibitory factor have been attributed to the modulation of macrophage functions although the molecular underpinnings have not been explored at a genome-wide scale. Herein, we investigated leukemia inhibitory factor–driven transcriptional changes in murine bone marrow–derived macrophages by RNA sequencing. In silico analyses revealed a selective and time-dependent remodeling of macrophage gene expression programs associated with lipid metabolism and cell activation. Accordingly, a subset of leukemia inhibitory factor–upregulated transcripts related to cholesterol metabolism and lipid internalization was validated by real-time quantitative polymerase chain reaction. This was accompanied by a leukemia inhibitory factor–enhanced capacity for lipid accumulation in macrophages upon incubation with oxidized low-density lipoprotein. Mechanistically, leukemia inhibitory factor triggered the phosphorylation (Y705 and S727) and nuclear translocation of the transcription factor STAT3 in bone marrow–derived macrophages. Consistent with this, ingenuity pathway analysis identified STAT3 as an upstream regulator of a subset of transcripts, including *Il4ra*, in leukemia inhibitory factor–treated macrophages. Notably, leukemia inhibitory factor priming enhanced bone marrow–derived macrophage responses to interleukin-4-mediated M2 polarization (i.e. increased arginase activity and accumulation of transcripts encoding for M2 markers). Conversely, leukemia inhibitory factor stimulation had no significant effect in bone marrow–derived macrophage responses to M1-polarizing stimuli (interferon-γ and lipopolysaccharide). Thus, our study provides insight into the transcriptional landscape of leukemia inhibitory factor–treated macrophages, shedding light on its role in lipid metabolism and M2 polarization responses. A better understanding of the regulatory mechanisms governing leukemia inhibitory factor–driven changes might help informing novel therapeutic approaches aiming to reprogram macrophage phenotypes in diseased states (e.g. cancer, atherosclerosis, and infection).

Keywords: cytokine, IL-4, inflammation, leukemia inhibitory factor (LIF), lipids, macrophage, metabolism, polarization, STAT3

1. Introduction

Leukemia inhibitory factor (LIF) is a member of the interleukin-6 (IL-6) family which includes other cytokines such as ciliary neurotrophic factor, cardiotrophin-like cytokine (CLC), cardiotrophin 1, IL-11, IL-27, and oncostatin M.[1] LIF is a heavily glycosylated protein which signals through engagement with the heterodimeric complex LIF receptor (LIFR) comprised of the glycoprotein 130 (common to all IL-6 family members) and the LIFR beta subunit.[2] Upon stimulation, LIF can activate a number of intracellular pathways (i.e. MAPK, PI3 K, YAP, mTOR, β-catenin, and JAK/STAT), among which signal transducer and activator of transcription 3 (STAT3)–dependent signaling is one of the best characterized.[3] As a pleiotropic cytokine, LIF has been reported to play a role in embryo implantation, tumor development, neuronal differentiation, lipid uptake, and inflammation.[4–8] ChIP-chip characterization of pituitary AtT-20 cells revealed the upregulation of a distinctive STAT3/glucocorticoid receptor–dependent cell defense transcriptional program upon LIF and glucocorticoid stimulation.[9,10] In addition, and consistent with a central role for LIF in placental cell function and normal pregnancy outcomes,[11] transcriptional profiling of 2 different human trophoblast cell lines identified a subset of invasion-associated genes induced upon LIF stimulation.[12,13] However, high-throughput analyses of the response to LIF in primary cells or cell types other than trophoblasts and pituitary corticotropes are still lacking.

Accumulating evidence indicates that LIF exerts a protective role during viral and bacterial infections. For instance, in the context of lung infections, LIF has been shown to promote tissue resistance to pathogen-induced damage in response to respiratory syncytial virus or *Escherichia coli*.[14–16] Additionally, LIF has been reported to inhibit human immunodeficiency virus 1 replication and transmission in vitro[17] and in vivo.[18]

In hematopoietic cells, LIF stimulation can favor the development of T regulatory cells (Tregs) with potential benefits in the

Received: July 12, 2024. **Revised:** July 24, 2024. **Accepted:** August 22, 2024. **Corrected and Typeset:** September 9, 2024

context of inflammatory pathologies such as multiple sclerosis and colitis.[19–21] Moreover, LIF modulates dendritic cell functions by promoting the development of semimature and tolerogenic subsets while inhibiting type I interferon (IFN), tumor necrosis factor (TNF), and IL-6 responses to 5′-cytosine-phosphate-guanine-3′ oligonucleotides.[22,23] Conversely, increased eosinophil activation and chemotaxis have been documented upon LIF treatment which could be detrimental in eosinophil-dependent airway disorders (e.g. asthma).[24] Of note, monocytes and macrophages have been identified as the primary hematopoietic cell types expressing LIFR.[25]

Macrophages are ubiquitous phagocytes essential for numerous immunological, inflammatory, and metabolic processes in homeostasis and disease while exhibiting a remarkable plasticity in their response to stimuli.[26] For example, classically activated macrophages (i.e. M1 macrophages) exhibit higher levels of glycolysis, pathogen killing, and TNF, IL-6, and IL-12 expressions following stimulation with proinflammatory signals such as IFNγ and bacterial lipopolysaccharide (LPS).[27,28] In contrast, alternatively activated macrophages (i.e. M2 macrophages) are elicited upon treatment with anti-inflammatory cues (e.g. IL-4) and play a paramount role in tissue repair and resolution of inflammation.[29,30] It has been reported that LIF is highly expressed in the tumor microenvironment which promotes the differentiation of resident macrophages toward an immunosuppressive phenotype.[31,32] Similarly, LIF has been shown to inhibit directly or indirectly inflammatory responses in IFNγ-primed human macrophages.[33,34] Despite this body of evidence, the overall transcriptional impact of LIF in macrophages has not been investigated.

Using a combination of in silico and experimental approaches in bone marrow–derived macrophages (BMDM), herein we show that LIF promotes transcriptional programs associated with lipid metabolism and macrophage alternative activation. More specifically, our study provides evidence that LIF-treated macrophages have an increased capacity for lipid accumulation and are poised to better respond to M2-polarizing stimuli.

2. Materials and Methods

2.1 Ethics statement

C57BL/6 mice were housed and handled according to a protocol approved by the Comité Institutionnel de Protection des Animaux (CIPA) of the INRS (CIPA #2102-01). This protocol respects procedures on good animal practice provided by the Canadian Council on Animal Care.

2.2 Reagents

Culture media and supplements were purchased from Wisent; cOmplete EDTA-free protease inhibitor and PhosSTOP phosphatase inhibitor tablets were purchased from Roche; STATTIC was purchased from Tocris; recombinant murine LIF was purchased from STEMCELL Technologies, and recombinant murine IFNγ was acquired through Cederlane; recombinant murine IL-4 was purchased from BioLegend; LPS was ordered from Sigma-Aldrich; oxidized low-density lipoprotein (Ox-LDL) from human plasma was obtained from Medix Biochemica; 4′,6-diamidino-2-phenylindole dilactate (DAPI) was purchased from Invitrogen; primary and secondary antibodies for western blotting, immunofluorescence, and flow cytometry were purchased from Cell Signaling Technologies, Sigma-Aldrich, and BioLegend.

2.3 Differentiation of murine BMDM

BMDM were generated from 6- to 8-week-old female C57BL/6 mice (Jackson Laboratory), as previously outlined.[35] Briefly, marrow was extracted from the bones of the hind legs, red blood cells were lysed, and progenitor cells were resuspended in BMDM culture medium supplemented with 15% L929 fibroblast-conditioned culture medium (LCCM). Nonadherent cells were collected the following day and were cultured for 7 d in BMDM culture medium supplemented with 30% LCCM with fresh medium replenishment at day 3 of incubation.

2.4 RNA purification and real-time quantitative polymerase chain reaction

Total cellular RNA was extracted with QIAzol (QIAGEN) according to the manufacturer's specifications. For samples processed for sequencing, RNA samples were further purified by using an RNeasy MinElute Cleanup Kit (QIAGEN), according to the manufacturer's recommendations. Finally, purified RNA concentration, purity, and integrity were assessed spectrophotometrically by using a NanoDrop 1000 instrument (Thermo Fisher Scientific) and a Bioanalyzer 2100 instrument with a Eukaryote Total RNA nanochip (Agilent Technologies).

For real-time quantitative polymerase chain reaction (RT-qPCR) analyses, approximately 0.5 to 1 µg of RNA was reverse transcribed using the LunaScript RT SuperMix Kit (New England Biolabs). RT-qPCR was performed with Luna qPCR Master Mix (New England Biolabs) using a QuantStudio 3 Real-Time PCR System (Thermo Fisher Scientific). Relative quantification of gene of interest expression was calculated using the comparative Ct method (ΔΔCt),[36] and relative expression was normalized to murine *Atcb* or *Rpl19*. Primers used for RT-qPCR analyses were designed using NCBI Primer-BLAST (http://www.ncbi.nlm.nih.gov/tools/primer-blast/) and are listed in Supplementary Table 4.

2.5 Library preparation and RNA sequencing data processing

RNA was quantified using Qubit (Thermo Fisher Scientific), and quality was assessed with the 2100 Bioanalyzer (Agilent Technologies). Transcriptome libraries were generated using the KAPA RNA HyperPrep (Roche) using a poly-A selection (Thermo Fisher Scientific). Sequencing was performed on the Illumina NextSeq 500, obtaining around 25 M single-end 75 bp reads per sample. Samples were submitted for Illumina next-generation sequencing to the IRIC Genomics Platform (Université de Montréal, QC, Canada). Adapter sequences and low-quality bases in the resulting FASTQ files were removed using Trimmomatic version 0.35,[37] and genome alignments were conducted using STAR version 2.7.1a.[38] Sequences were aligned to the mouse genome version GRCm38 with gene annotations from Gencode version M25 based on Ensembl 100. As part of quality control, sequences were aligned to several different genomes to verify that there was no sample contamination. Expression levels were obtained as gene read counts from STAR as well as estimated using RSEM[39] to obtain gene and transcript level expression in reads per transcripts per million for these stranded RNA libraries. DESeq2 version 1.30.1[40] was then used to normalize gene read counts and compute differential expression between the various experimental conditions. Significant gene sets were chosen according to a false discovery rate (FDR) cutoff of 5% ($P.adj < 0.05$). Computing both a hierarchical sample clustering based on Pearson correlation of normalized log read counts and a principal component analysis shows that samples behave as expected, with no obvious outlier, as well as good consistency among replicates.

2.6 Ingenuity pathway analysis

Enrichment of transcripts showing differential abundance in specific functional networks was determined using ingenuity pathway analysis (IPA) (QIAGEN) by comparing significantly regulated gene sets against the entire sequenced data sets. Within the IPA application, statistical significance was calculated using a right-tailed Fisher Exact test, and *P*-values were adjusted for multiple hypothesis testing using the Benjamini–Hochberg method to arrive at an FDR.

2.7 BMDM stimulation

Macrophages were plated 1 d prior to stimulation with LIF and allowed to adhere O/N at 37 °C, 5% CO_2. On the following day, cultures were stimulated or not with 50 ng/mL LIF for the indicated times. When applicable, cells were stimulated 24 h following addition of LIF inoculation with 100 U/mL IFNγ (Cederlane #CLCYT651) and 10 ng/mL LPS (Sigma-Aldrich # L2630) or 20 ng/mL IL-4 (BioLegend #574302) for 24 h.

2.8 Ox-LDL uptake and lipid droplet staining

Macrophages were plated on glass coverslips and stimulated with LIF for 24 h, as described above. Cells were serum-starved for 4 h, and then, fresh culture medium supplemented or not with 100 μM Ox-LDL was added to cultures for an additional 24 h, as reported.[41] BMDM were fixed in 2% paraformaldehyde (PFA) in phosphate-buffered saline (PBS) and stained with 10 μg/mL BODIPY 493/503 dye (4,4-Difluoro-1,3,5,7,8-Pentamethyl-4-Bora-3a,4a-Diaza-s-Indacene, Invitrogen, #D3922), as described.[42] Cells were permeabilized using 0.1% Triton X-100 in PBS, and nonspecific surface binding was blocked in blocking buffer (1% bovine serum albumin [BSA], 5% skim milk, and 5% FBS in PBS) for 20 min at room temperature (RT). Nuclei were stained with 2 μM DAPI (Invitrogen, #D21490). Coverslips were mounted on slides with Fluoromount-G (Southern Biotech). Samples were visualized with the 63× objective, and sequential z-stack images were captured using a Zeiss LSM780 system equipped with a 30 mW 405 nm diode laser and a 25 mW 458/488/514 argon multiline laser mounted onto a Zeiss Axio Observer Z1 and operated with Zen 2011 software (Zeiss). BODIPY 493/503 and DAPI signal intensity was quantified by using ImageJ (National Institutes of Health).

2.9 Western blot analysis

Cells were lysed in RIPA lysis buffer (25 mM Tris [pH 7.6], 150 mM NaCl, 1% Triton-X 100, 0.5% sodium deoxycholate, 0.1% SDS) supplemented with cOmplete EDTA-free protease inhibitor, PhosSTOP phosphatase inhibitor tablets, and 10 mM 10-phenanthroline monohydrate (Sigma-Aldrich), and samples were prepared for western blotting as described.[43] Membranes were probed with the following primary antibodies: rabbit anti-phospho-STAT3 (Y705) (clone D3A7, #9145), rabbit anti-phospho-STAT3 (S727) (clone D8C2Z, #94994), mouse anti-STAT3 (clone 124H6, #9139), rabbit-anti-arginase-1 (polyclonal, #9819), rabbit anti-iNOS (polyclonal, #2982), rabbit anti-phospho-STAT6 (Y641) (clone D8S9Y, #56554), rabbit anti-STAT6 (clone D3H4, #5397), and mouse anti-β-actin (clone 8H10D10, #3700) (Cell Signaling Technologies). Membranes were then incubated with the following horseradish peroxidase (HRP)–conjugated antibodies: goat anti-rabbit IgG (#A0545) and goat anti-mouse IgG (#A4416) (Sigma-Aldrich). Proteins were then detected by chemiluminescence using Clarity Western ECL substrate (Bio-Rad) and exposing membranes to autoradiography film (Denville Scientific).

2.10 Immunofluorescence and confocal microscopy

BMDM were seeded onto glass coverslips in 24-well plates overnight. At the indicated time points, cultures were rinsed with PBS 3 times and then fixed with 2% PFA in PBS for 15 min at RT. Cells were permeabilized with methanol for 10 min at 4 °C. Samples were incubated in blocking solution (5% normal goat serum, 0.3% Triton X-100, 0.05% sodium azide in PBS) supplemented with 10 μg/mL rat anti-mouse CD16/32 (Fcγ III/II) (clone 93; #101302) (BioLegend) for 1 h at RT. Samples were then incubated O/N at 4 °C with a rabbit anti-phospho-STAT3 (Y705) (clone D3A7, #9145) (Cell Signaling Technologies) diluted in antibody buffer (1% BSA, 0.5% Triton X-100 in PBS). Samples were stained with a goat anti-rabbit IgG (H + L) conjugated to Alexa Fluor 488 (polyclonal, #A-11034, Invitrogen) diluted in antibody buffer supplemented with 2 μM DAPI (Invitrogen, #D21490) for 1 h at RT. Coverslips were mounted onto slides with Fluoromount-G (#00-4958-02, Invitrogen). Samples were visualized with the 63× objective of an LSM780 Zeiss confocal microscope; image acquisition and processing were carried out using ZEN software.

2.11 Flow cytometry staining

BMDM were detached from plates using ice-cold PBS with 5 mM EDTA and then washed once with FACS buffer (0.1% BSA in PBS). Fc receptors were blocked with rat anti-mouse CD16/32 (Fcγ III/II) (clone 93; #101302) (BioLegend) and then probed with the following antibodies for 30 min on ice: rat APC-anti-mouse CD124 (IL-4Rα) (clone I015F8, #144807) and rat FITC-anti-mouse CD206 (MMR) (clone #C068C2, #141703) (BioLegend). Isotype-matched APC-conjugated rat IgG2a, κ (clone RTK2758, #400511) or FITC-conjugated rat IgG2b, and κ (clone RTK2758, #400505) (BioLegend) were included to control for nonspecific staining. After staining, cells were washed once with FACS buffer. Samples were acquired using a BD LSRFortessa (BD Biosciences), and data were analyzed using FlowJo software (Tree Star).

2.12 Viability assay

Viability of BMDM following STATTIC (Tocris) treatment was determined by the resazurin assay as described.[44] Briefly, cells were treated with 2-fold serially diluted STATTIC (starting at 40 μM) or an equivalent volume of DMSO (vehicle) for 24 h at 37 °C, 5% CO_2. Cultures were then incubated with culture medium supplemented with 0.025% resazurin for an additional 6 h. Optical density was measured using a Multiskan GO (Thermo Fisher Scientific) at 600 and 570 nm. Absorbance at 600 nm was subtracted from readings at 570 nm. Viability was calculated as a percentage of readings from DMSO-treated cultures.

2.13 Nitrite measurement (Griess reaction)

Culture supernatants were collected from BMDM cultures following treatment, and nitric oxide (NO) production was measured using the Griess reaction to generate nitrites, as previously described.[45] Absorbance was measured at 548 nm, and nitrite concentrations were calculated using linear regression obtained from serial dilution of sodium nitrite standards.

2.14 Arginase enzymatic activity

Arginase enzymatic activity was measured as previously described.[46] Briefly, BMDM cultures were lysed in 0.1% Triton X-100 supplemented with cOmplete EDTA-free protease inhibitor for 15 min at RT. Lysates were diluted with a solution containing

50 mM Tris (pH 7.5) and 5 mM $MnCl_2$. Samples were incubated at 56 °C for 7 min; then, 250 mM L-arginine was added. Mixtures were incubated for 37 °C for 1 h. Enzymatic reaction was stopped by adding an equal volume of Stop Solution (H_3PO_4:H_2SO_4:H_2O [1:3:7 ratio]). Alpha-isonitrosopropiophenone was added (0.6% final), and samples were incubated at 95 °C for 1 h. After heating, samples were cooled down, and optical density was measured at 540 nm with a Multiskan GO (Thermo Fisher Scientific). Arginase enzymatic activity was calculated using values obtained from urea standards and expressed as milli-enzyme units per million cells (mU/10^6 cells).

2.15 IL-10 ELISA

Soluble IL-10 in the supernatants from LIF-treated, LPS-treated, and control BMDM cultures was assessed using the ELISA capture IL-10 antibody (#504902) and ELISA detection IL-10 biotinylated antibody (#505004) from BioLegend. Concentrations were calculated from standard curves generated using linear regression analysis of data obtained from serial dilutions with recombinant murine IL-10 (BioLegend, #575809).

2.16 Statistical analysis

Where applicable, data are presented as mean (SD). Statistical significance was determined using analysis of variance. Differences were considered significant when $^{***}P < 0.001$, $^{**}P < 0.01$, and $^{*}P < 0.05$.

3. Results

3.1 LIF induces distinct transcriptional changes in macrophages

LIF has been shown to modulate gene expression in macrophages.[31,32] However, LIF-driven transcriptomic reprogramming of macrophages has not been investigated. To address this, we first set out to assess transcriptome-wide changes in mRNA abundance in murine primary macrophages following LIF stimulation. BMDM cultures were incubated with recombinant LIF or left untreated for 4, 8, or 24 h. Total mRNA was collected at each time point and subjected to RNA sequencing (RNA-seq). Downstream bioinformatic analyses revealed a gradual increase in the number of significantly regulated genes (Fig. 1A), ranging from 38 (37 up, 1 down) at 4 h and 68 (65 up, 3 down) at 8 h up to 544 (325 up, 219 down) at 24 h poststimulation compared to unstimulated control conditions (Supplementary Table 1A to C). These data sets indicate that LIF stimulation favors the upregulation of a subset of macrophage mRNAs starting at early time points while inhibiting the accumulation of a different group of transcripts later during treatment.

To identify differentially regulated canonical pathways potentially linked to transcriptional changes upon BMDM treatment with LIF, we used IPA. In total, 54 canonical pathways were predicted to be significantly activated after a 24 h LIF stimulation, while only 10 and 19 pathways were identified at 4 and 8 h post-LIF stimulation, respectively (Supplementary Table S2A to C). Among these canonical pathways, several categories were of particular interest in the context of macrophage biology, notably cytokine and lipid mediator signaling (IL-4, IL-13, and IL-6-type cytokines; pathogen-induced cytokine storm; eicosanoid signaling; and TREM1 signaling), macrophage polarization (alternative and classical activation signaling pathways), and macrophage biological processes (phagosome formation and cholesterol biosynthesis) (Fig. 1B). Consistent with IPA data indicative of LIF-driven modulation of immune responses and lipid metabolism in macrophages, several mediators of cell activation (e.g. *Cd40*, *Tarm1*, and *Sting1*), tissue repair (e.g. *Fn1* and *Ptger4*), cytokines and cytokine receptors (e.g. *Il-10*, *Il1b*, and *Il4ra*), and chemokines and chemokine receptors (e.g. *Ccl12*, *Ccl2*, *Ccl8*, *Ccr5*, and *Cxcl10*) were among differentially expressed genes manually curated under "Immune Response" (Fig. 2, left panel). Similarly, transcripts encoding for lipid receptors (e.g. *Cysltr1*, *Ffar2*, *Ldlr*, and *Ltb4r1*) and enzymes involved in fatty acid, phospholipid, and cholesterol metabolism (e.g. *Cyp51*, *Mvd*, *Enpp6*, *Plbd1*, *Plppr3*, *Soat2*, and *Sqle*) were also identified in the upregulated data set manually curated under "Lipid Metabolism and Signaling" (Fig. 2, right panel).

In line with the kinetics of transcript downregulation upon LIF treatment (Fig. 1A; Supplementary Table 1A to C), IPA did not identify any canonical pathways predicted to be inhibited at 4 and 8 h poststimulation while only 5 were detected at 24 h (Supplementary Table 2D and Fig. 1A). Such pathways comprised transcripts associated with cell migration (e.g. *Cx3cr1*, *Cxcl14*, and *Vegfa*), oxidative response (e.g. *Enc1* and *Mgst2*), and immune response (e.g. *Cav1*, *Clec7a*, *Havcr2*, *Mmp12*, and *Klrb1c*, etc.) (Supplementary Fig. 1B). Taken together, in silico analyses of our transcriptomic data provide evidence of LIF-driven selective remodeling of gene expression programs predicted to modulate macrophage polarization, immune activation, and lipid metabolism.

3.2 LIF stimulation modulates lipid metabolism in macrophages

LIF has been reported to modulate lipid metabolism by promoting[47] or inhibiting lipogenesis.[48] Consistent with IPA-predicted activation of canonical pathways related to lipid metabolism in BMDM (Figs. 1B and 2; Supplementary Table 2C), LIF treatment upregulated the expression of transcripts associated with cholesterol biosynthesis (e.g. *Cyp51*, *Dhcr24*, *Fdps*, *Hsd17b7*, *Idi1*, *Mvd*, *Pmvk*, and *Sqle*) and esterification (e.g. *Soat2*) as well as lipid mediator signaling, fatty acid and phospholipid metabolism, and trafficking (e.g. *Atp8b1*, *Cysltr1*, *Enpp6*, *Fads3*, *Ffar2*, *Ldlr*, *Lipg*, *Lpar1*, *Ltb4r1*, *Naaa*, *Plbd1*, *Plppr3*, *Ptger3*, and *Ptger4*) (Fig. 2 and 3A). Previous reports have highlighted the central role of LIF in modulating lipid metabolism, including lipid uptake.[8] Hence, we set out to examine the foam cell formation capacity of Ox-LDL[49] in the presence or absence of LIF using BODIPY staining and confocal microscopy. Increased lipid accumulation was detected upon LIF treatment (Fig. 3B, left panel). Lipid signal quantification indicated a 9.2-fold increase in normalized BODIPY intensity of LIF-treated macrophages compared to unstimulated controls (Fig. 3B, top right panel). In addition, LIF enhanced lipid accumulation in Ox-LDL-treated BMDM cultures (Fig. 3B, left panel), as evidenced by a 1.8-fold increase in normalized BODIPY signal intensity in cells primed with LIF compared to unprimed Ox-LDL-treated controls (Fig. 3B, bottom right panel). In all, this set of experiments indicates that LIF treatment activates transcriptional programs associated with lipid metabolism with a concomitant upregulation of macrophage capacity for lipid accumulation.

3.3 LIF activates STAT3-dependent transcriptional programs in macrophages

IPA analyses of LIF-induced transcriptional changes predicted the activation of several upstream transcriptional regulators, including STAT3 among those with the highest activation Z-score (Supplementary Table 3). This transcription factor modulates macrophage activation and polarization in a context dependent manner by regulating the expression of inflammatory effectors

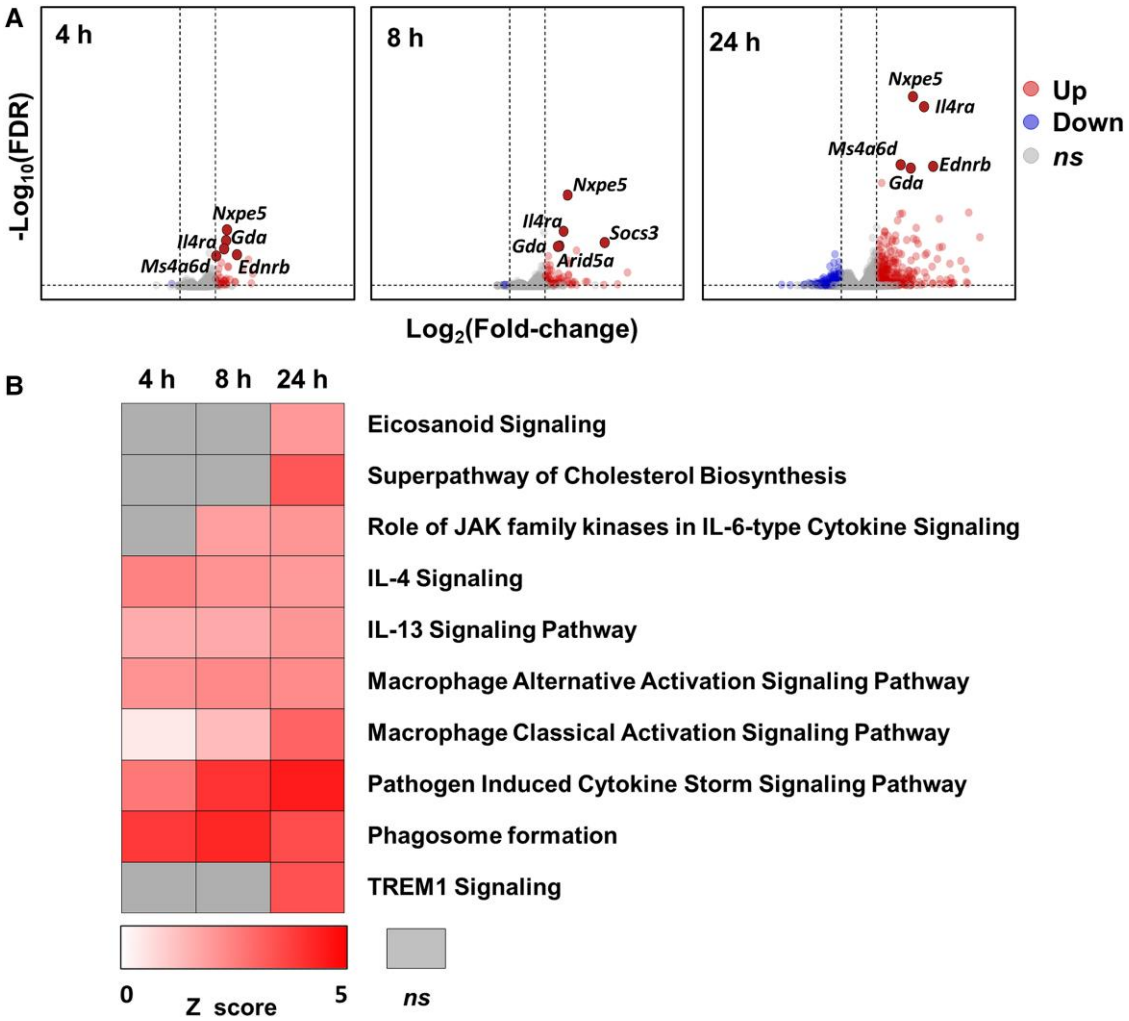

Fig. 1. LIF induces distinct transcriptional changes in macrophages. BMDM cultures were treated or not with 50 ng/mL recombinant LIF. Total mRNA was extracted 4, 8, and 24 h poststimulation and subjected to RNA-seq analysis. (A) Volcano plots showing the differentially expressed genes in BMDM following LIF treatment at the indicated times compared to unstimulated cultures. Differentially expressed genes were identified by DESeq2 with an FDR of 5% and a $\log_2$ expression fold-change ≥ 1.0. The top 5 upregulated differentially expressed genes by FDR are highlighted at the indicated time points. Up, significantly upregulated transcripts. Down, significantly downregulated transcripts. *ns*, nonsignificantly regulated transcripts. (B) IPA activation scores (Z) of predicted time-dependent upregulation ($Z \geq 2$) of canonical pathways following LIF treatment. *ns*, not significant. Heat maps were generated using Morpheus (Broad Institute; https://software.broadinstitute.org/morpheus/index.html). Analyses were carried out on data generated from 3 independent biological replicates.

(e.g. *Il10*, *Il4rα*, *Il6*, *Socs3*, and *Tnf*) and profibrotic factors (e.g. *Igf*, *Fn*, and *Tgfb1*) that can alleviate tissue damage.[50,51] Phosphorylation of STAT3 at Y705 is a requirement for its dimerization and translocation to the nucleus (i.e. STAT3 canonical activation).[52] In addition, noncanonical STAT3 phosphoactivation at S727 promotes breast, lung, and gastric carcinogenesis by favoring the expression of mitochondrial- and nuclear-encoded transcripts.[53–56] LIF-inducible STAT3 phosphorylation has been reported in different cell types, including human monocyte-derived macrophages.[34] To determine whether treatment with LIF activated STAT3 in BMDM, we monitored the phosphorylation status at residues Y705 and S727 by western blotting (Fig. 4A). Phosphorylation levels at both residues were induced rapidly after the addition of LIF, especially between 0.08 (15 min) and 1 h. Although phosphorylation levels receded beyond 1 h posttreatment, phosphorylation at residue Y705 remained higher in LIF-stimulated cells compared to unstimulated control cultures up to 24 h. Increased and sustained phosphorylation of STAT3 at Y705 was also observed by confocal microscopy which coincided with its nuclear localization upon exposure to LIF (Fig. 4B). In all, these data indicate that LIF treatment induces STAT3 phosphorylation and nuclear translocation in BMDM.

Consistent with the activation of the STAT3 signaling pathway, several transcripts predicted by IPA to be STAT3 regulated (Supplementary Table 3) were significantly induced in BMDM upon LIF treatment (Fig. 4C). Changes in expression levels of 3 different transcripts, namely, *Il4ra*, *Socs3*, and *Timp1*, were validated by RT-qPCR analyses (Fig. 4D). These transcriptional targets have also been associated with IL-10-dependent STAT3 activation.[57] To evaluate the possible contribution of endogenous IL-10 production in LIF-treated macrophages, we measured IL-10 accumulation in BMDM supernatants. Accordingly, very low or below detection levels of secreted IL-10 were found in macrophages treated or not with LIF (Supplementary Fig. 2). Thus, our results suggest that LIF activation of STAT3 is likely IL-10 independent.

To confirm STAT3-mediated transcription of these LIF-induced transcripts, we employed a biochemical approach using STATTIC, an inhibitory compound reported to block STAT3 nuclear

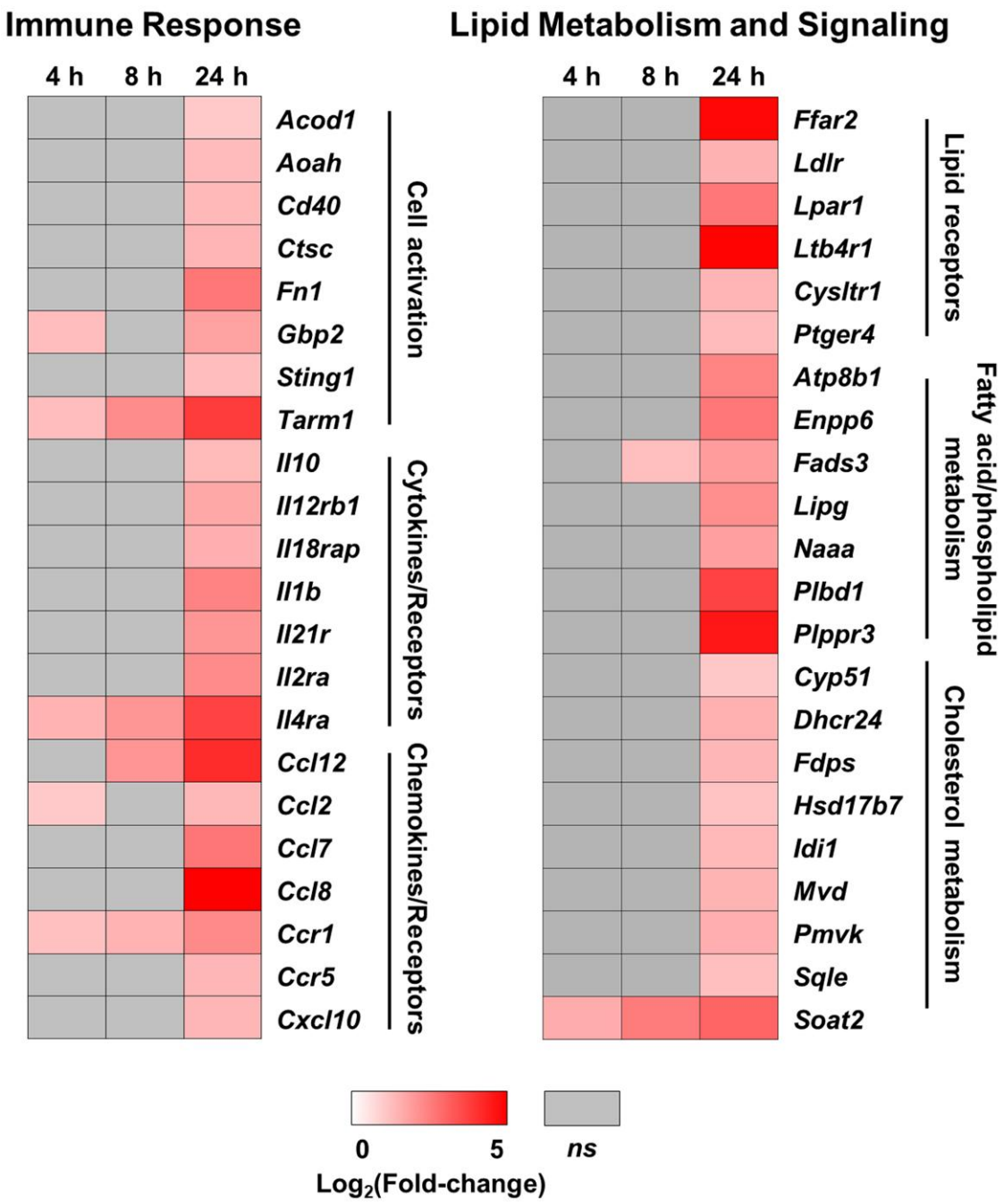

Fig. 2. LIF stimulation upregulates different subsets of transcripts associated with immune functions and lipid metabolism and signaling in macrophages. Within the different enriched categories identified by IPA (see Fig. 1B and Supplementary Table 2A to C), subsets of differentially expressed genes related to immune responses or lipid metabolism and signaling were grouped according to biological functions. Shown here are heat maps of Log_2(FC) of individual genes. *ns*, not significant. Heat maps were generated using Morpheus (Broad Institute). Analyses were carried out on data generated from 3 independent biological replicates.

translocation and phosphorylation specifically at residue Y705.[58] Toxicity assays revealed that doses ≤ 2.5 μM do not significantly affect BMDM viability after 24 h of exposure (Supplementary Fig. 3). We then performed a dose-response experiment to assess the efficacy of the inhibitor by western blotting. LIF-induced STAT3 phosphorylation at residue S727 was not inhibited at any STATTIC concentration tested, confirming a specific activity of the compound toward residue Y705 (Fig. 5A). Although a dose of 5 μM showed a total inhibition of LIF-induced STAT3 phosphorylation at residue Y705, the toxicity of the compound (Supplementary Fig. 3) precluded its use. On the other hand, a concentration of 2.5 μM partially inhibited STAT3 phosphorylation at Y705 (Fig. 5A) while not demonstrating overt toxicity in BMDM cultures (Supplementary Fig. 3). Pretreatment with 2.5 μM STATTIC not only substantially blocked STAT3 phosphorylation at Y705 but also inhibited its translocation into the cell nucleus as revealed by confocal microscopy (Fig. 5B). Importantly, exposure to STATTIC prior to stimulation significantly inhibited LIF-induced increase of *Il4ra*, *Socs3*, and *Timp1* transcript levels (Fig. 5C). In line with RT-qPCR analyses, STATTIC reduced cell

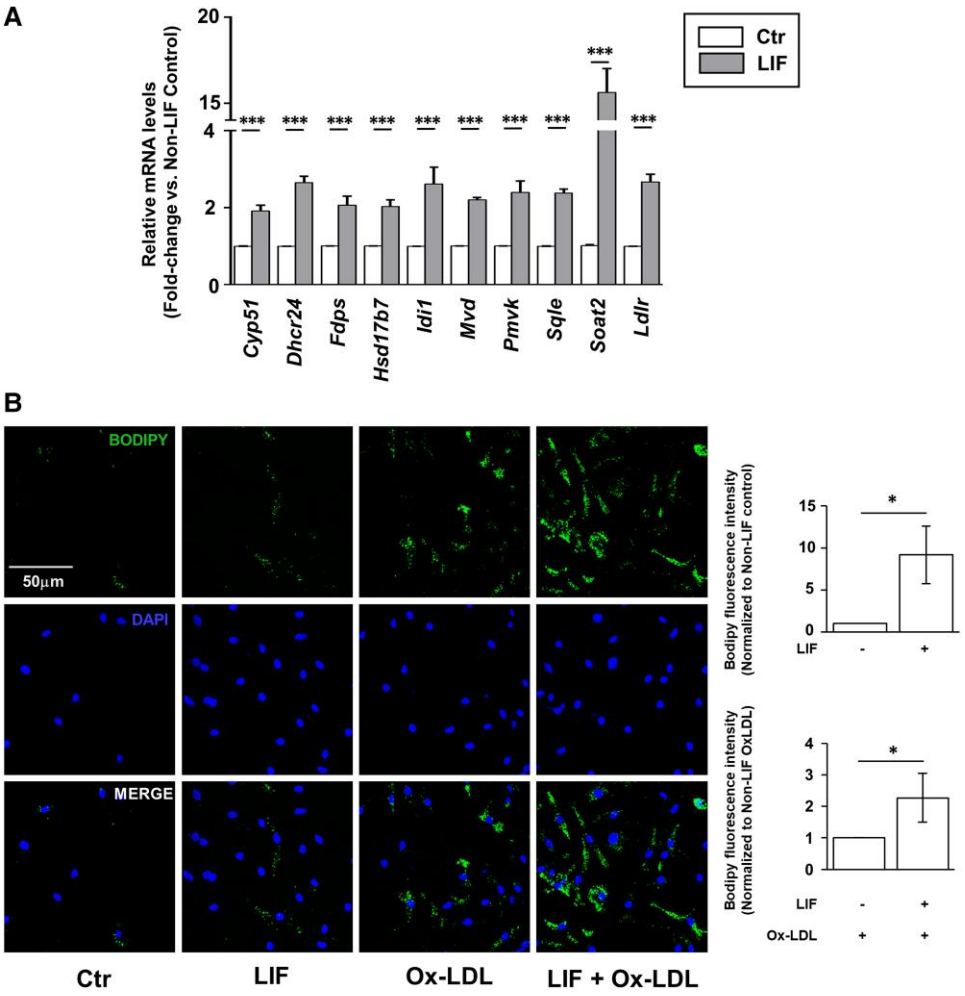

Fig. 3. LIF stimulation modulates lipid metabolism in macrophages. (A) BMDM cultures were stimulated or not with LIF for 24 h. Total mRNA was collected and subjected to RT-qPCR analyses for selected transcripts linked to lipid and cholesterol metabolism (normalized to *Actb*). Data are plotted as means (SD) calculated from 3 independent biological replicates. (B) BMDM cultures were stimulated or not with LIF for 24 h and then serum starved for 4 h. Fresh culture medium supplemented or not with 100 μM Ox-LDL was added to cultures for an additional 24 h. Samples were fixed, stained with BODIPY 493/503 and DAPI, and processed for confocal microscopy. Shown here are representative images of lipid droplet accumulation within macrophages under indicated conditions (left panel). Fluorescence intensity of lipid droplets stained with BODIPY 493/503 was measured by ImageJ and normalized to DAPI fluorescence intensity (right panel). Data are plotted as means (SD) calculated from 3 independent biological replicates. Differences were considered significant when $^{***}P < 0.001$, $^{**}P < 0.01$, and $^{*}P < 0.05$.

surface expression of the *Il4ra*-encoded IL-4 receptor alpha subunit (IL-4Rα) in both unstimulated and LIF-stimulated BMDM cultures (Fig. 5D and E). Taken together, this set of experiments provides evidence that LIF triggers a STAT3-mediated transcriptional signature in macrophages.

3.4 LIF priming enhances IL-4-mediated M2 macrophage polarization

It has been reported that LIF skews macrophage activation toward immunosuppressive phenotypes (i.e. tumor-associated macrophages).[31–34] Interestingly, IPA of our RNA-seq data sets identified canonical pathways associated with both macrophage classical and alternative signaling pathways in LIF-treated macrophages when compared to unstimulated controls (Fig. 1B; Supplementary Table 2). We therefore tested whether priming of BMDM culture with LIF would alter their response to M1- and/or M2-polarizing stimuli (i.e. LPS and IFNγ and IL-4, respectively).[27] We first measured transcript levels of 4 M1-associated genes (i.e. *Nos2*, *Cd80*, *Cd86*, and *Cxcl10*) by RT-qPCR. Stimulation of BMDM cultures with LIF alone did not lead to significant changes in the expression of any M1-related transcripts tested compared to unstimulated controls (Fig. 6A). Treatment with LPS and IFNγ robustly induced the accumulation of *Nos2*, *Cd80*, *Cd86*, and *Cxcl10* mRNAs, as previously reported.[27] However, priming with LIF did not affect the magnitude of induction (Fig. 6A, left panel). Out of these set of 4 genes, only *Cd86* showed a small significant decrease in LIF-primed macrophages, but this marginal difference may not ultimately lead to significant changes in CD86 protein expression in this context (Fig. 6A, left panel). In line with our RT-qPCR data, increased iNOS expression and soluble nitrite accumulation were observed in macrophages treated with LPS and IFNγ although no differences were observed when cells were primed or not with LIF (Fig. 6D and E). Thus, LIF does not affect LPS- and IFNγ-driven M1 polarization of macrophages.

We next set out to elucidate whether in agreement with our IPA data (Fig. 1B, Supplementary Table 2) LIF promoted macrophage responses to the M2-polarizing cytokine IL-4.[27] To address this, the expression of M2-associated genes was monitored in BMDM cultures exposed to LIF or left untreated prior to stimulation

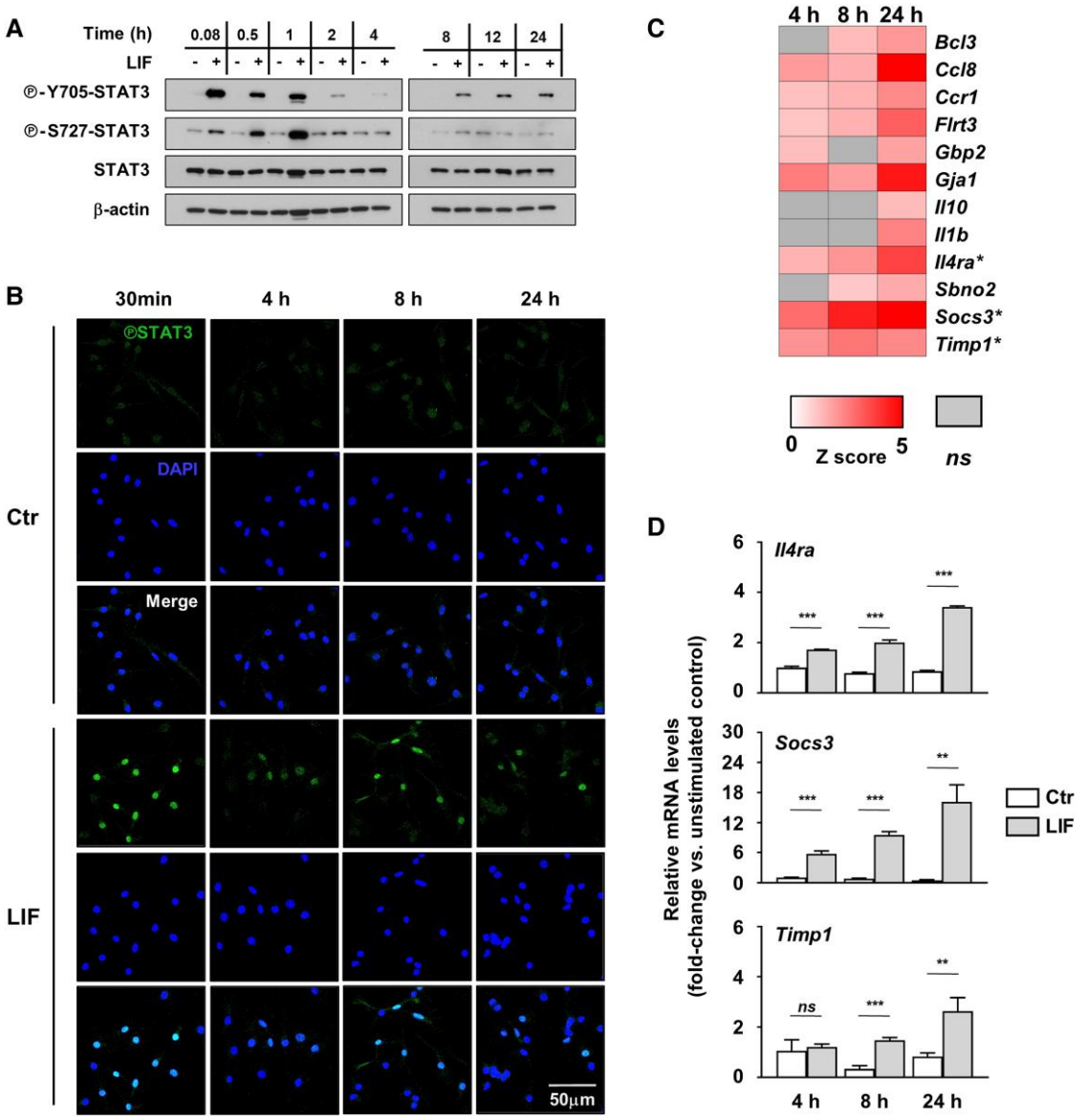

Fig. 4. LIF triggers STAT3 phosphorylation and nuclear localization leading to the activation of a STAT3-dependent transcriptional program. IPA identified STAT3 as an upstream transcriptional regulator (see Supplementary Table 3A to C) in BMDM upon LIF treatment. BMDM cultures were stimulated or not with LIF at the indicating times. (A) Phosphorylation of STAT3 at Y705 and S727 and total protein levels were monitored by western blotting. Total amounts of β-actin were used as a loading control. (B) Nuclear localization of phospho-STAT3 (Y705) was assessed by confocal microscopy by colocalization with DAPI signal. (C) Heat map of transcripts identified by IPA as transcriptionally regulated by STAT3. *ns*, not significant. Heat maps were generated using Morpheus (Broad Institute). (D) Total mRNA collected from LIF-stimulated and unstimulated BMDM cultures was subjected to RT-qPCR analyses for selected transcripts (*Il4ra*, *Socs3*, and *Timp1*) predicted to be transcriptionally regulated by STAT3. Data are plotted as means (SD) calculated from 3 independent biological replicates. Differences were considered significant when $^{***}P < 0.001$, $^{**}P < 0.01$, and $^{*}P < 0.05$.

with IL-4. As expected, treatment with IL-4 alone augmented mRNA levels of *Arg1*, *Chil3*, *Mrc1*, and *Retnla* (Fig. 6A, right panel). Interestingly, LIF alone led to an increase in *Mrc1* and *Retnla* transcripts (Fig. 6A, right panel) which was independent of STAT6 activation as determined by lack of STAT6 phosphorylation upon LIF stimulation (Supplementary Fig. 4). Conversely, LIF priming potentiated macrophage responses to IL-4 stimulation as evidenced by a significant enhancement of all 4 selected M2 markers compared to IL-4 alone (Fig. 6A, right panel). In turn, treatment with either LIF or IL-4 alone induced cell surface expression of *Mrc1*-encoded mannose receptor CD206 in BMDM cultures, while priming with LIF followed by IL-4 led to the strongest increase in its expression (Fig. 6B and C). Similarly, LIF priming was required for *Arg1*-encoded arginase 1 (ARG1) induction (Fig. 6D) and enhanced arginase activity (Fig. 6F) upon IL-4 treatment in macrophages. Taken together, these data indicate that LIF potentiates IL-4-driven polarization of M2 macrophages.

4. Discussion

LIF is a pleiotropic cytokine of the IL-6 family, as evidenced by its central regulatory role in a wide array of cell types (e.g. trophoblasts, neurons, adipocytes, T cells, dendritic cells, monocytes, and macrophages)[3] and biological processes (e.g. blastocyst implantation, nervous system development, bone metabolism, tissue regeneration, immune activation, and tumorigenesis).[2] Accumulating evidence indicates that LIF modulates macrophage functions in healthy and diseased states.[31–34] Surprisingly,

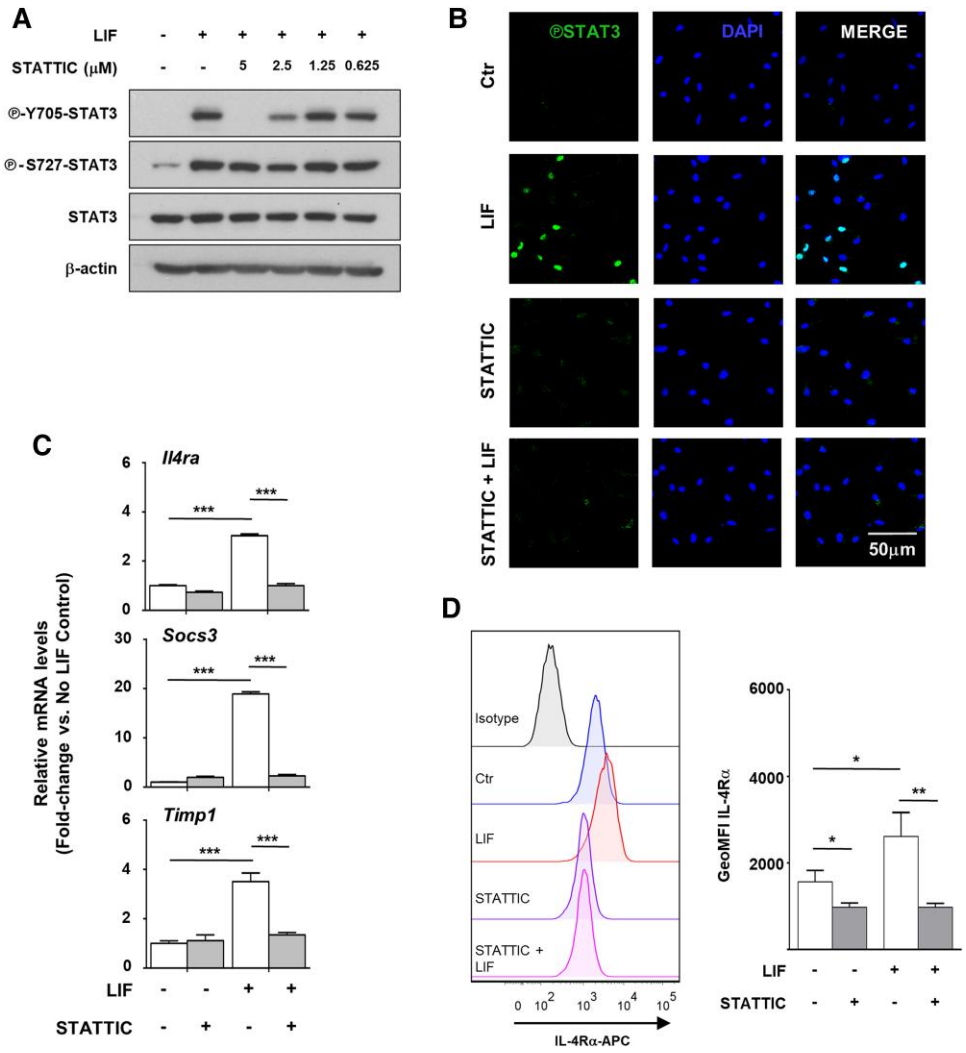

Fig. 5. Inhibition of STAT3 ablates LIF-induced STAT3-mediated transcription. (A) BMDM cultures were pretreated with different doses of STATTIC (2-fold serial dilutions starting at 5 μM) or vehicle (DMSO) for 1 h. Cells were then treated or not with LIF for 30 min. Phosphorylation of STAT3 at Y705 and S727 and STAT3 total protein levels were monitored by western blotting. Total amounts of β-actin were used as a loading control. (B) BMDM cultures were pretreated with 2.5 μM STATTIC or an equivalent volume of DMSO for 1 h. Cells were then stimulated or not with LIF for 30 min. The inhibitory effects of STATTIC on STAT3 phosphorylation (Y705) and nuclear localization were assessed by colocalization with DAPI signal. (C) BMDM cultures were pretreated with 2.5 μM STATTIC or an equivalent volume of DMSO for 1 h. Cells were then stimulated or not with LIF for 8 h. Total mRNA was collected and subjected to RT-qPCR analyses for selected transcripts (*Il4ra*, *Socs3*, and *Timp1*) predicted to be transcriptionally regulated by STAT3. (D) BMDM cultures were pretreated with 2.5 μM STATTIC or an equivalent volume of DMSO for 1 h. Cells were then stimulated or not with LIF for 24 h. Surface expression of IL-4Rα was monitored by flow cytometry. An isotype-matched APC-conjugated antibody was included to control for nonspecific staining (left panel). Geometric mean fluorescence intensity of IL-4Rα staining measured by flow cytometry was plotted for each condition (right panel). Where applicable, data are plotted as means (SD) calculated from 3 independent biological replicates. Differences were considered significant when $^{***}P < 0.001$, $^{**}P < 0.01$, and $^{*}P < 0.05$.

transcriptome-wide characterization of macrophage responses to LIF is lacking. Herein, we report that LIF induces wide but distinct transcriptional changes in primary murine macrophages leading to alterations in lipid metabolism and enhanced IL-4-mediated polarization.

Contrasting reports show divergent roles for LIF in lipid metabolism. For instance, adipocyte differentiation is favored by LIF through the MAPK-driven activation of CREB, C/EBPβ, and C/EBPϵ.[59–61] Conversely, hydrocortisone-induced adipocyte differentiation is impaired in stromal cells treated with cytokines of the IL-6 family, including LIF.[62] Moreover, LIF-induced cachexia occurs via inhibition of hepatic lipogenesis and lipid uptake via the STAT3-dependent downregulation of PPARα, a master regulator of lipid metabolism, in a model of tumor transplantation.[48] Interestingly, it has also been reported that LIF stimulation increases hepatic lipid uptake in cholesterol-fed rabbits and inhibits atherosclerotic lesion development.[8] Additionally, Marshal et al.[47] showed that LIF treatment can induce metabolic changes in cultured adipocytes including augmented fatty acid synthesis.

Although a previous study indicated that LIF stimulation does not influence the lipid uptake capacity of the murine macrophage cell line J774,[63] our data provides evidence that LIF promotes the expression of a transcriptional program associated with lipid biogenesis and uptake in murine primary macrophages. Similar results were reported by Pasquin et al.[41] who investigated the role of CLC, another IL-6 family member, in the formation of foam cells. The authors concluded that CLC induces: *i*) the expression of the scavenger receptor SR-A1 (*Msr1*), *ii*) macrophage uptake of acetylated LDL, and *iii*) triglyceride accumulation in BMDM.

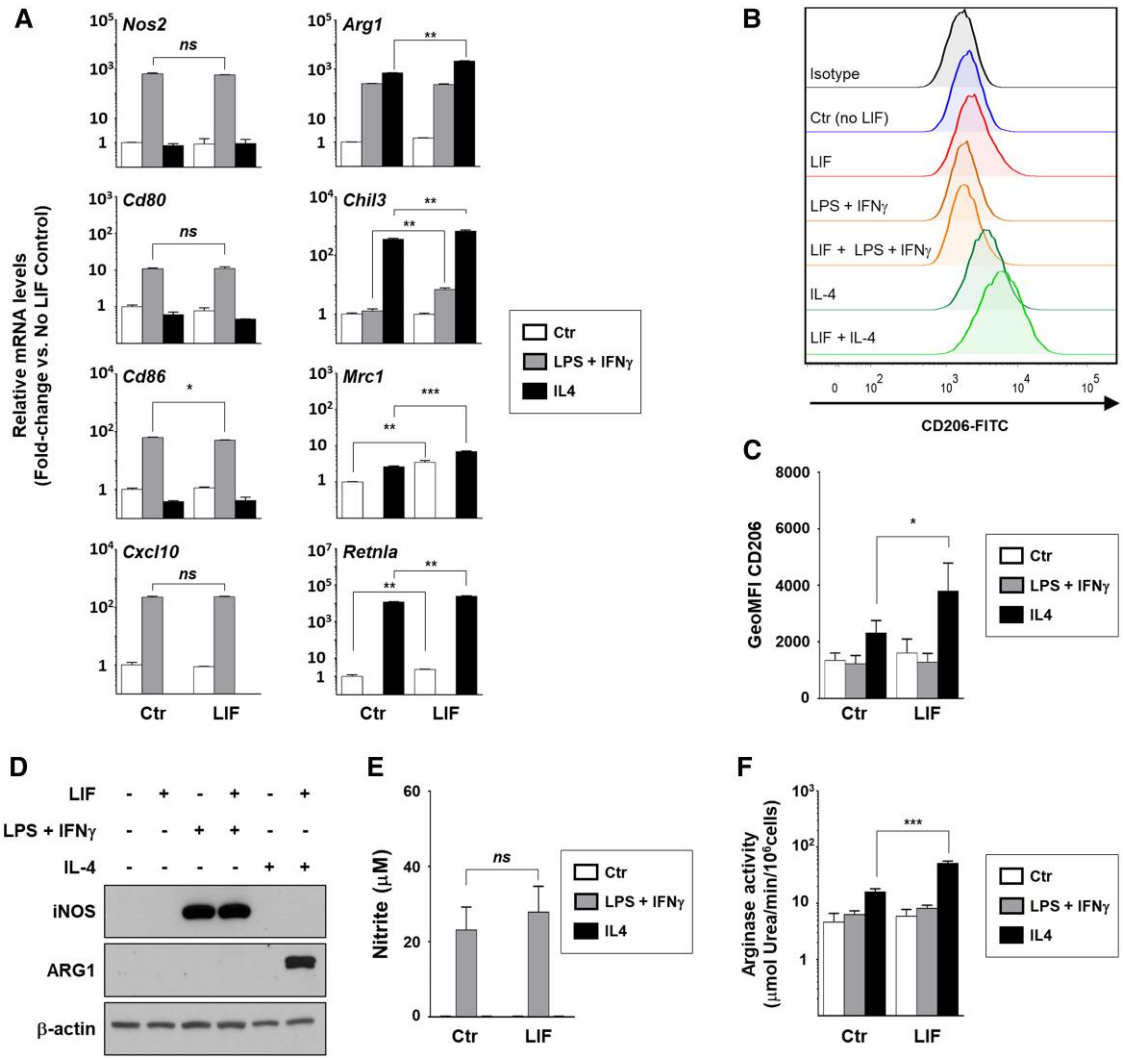

Fig. 6. LIF priming enhances IL-4-mediated M2 macrophage polarization. BMDM cultures were primed or not with LIF for 24 h and then stimulated or not with M1-promoting LPS and IFNγ, or M2-inducing IL-4 for an additional 24 h. (A) Total mRNA was collected and subjected to RT-qPCR analyses for markers associated with M1 (*Nos2*, *Cd80*, *Cd86*, and *Cxcl10*) or M2 (*Arg1*, *Chil3*, *Mrc1*, and *Retnla*) polarized macrophages. Normalized expression levels are reported as fold-change compared to unstimulated controls (i.e. *no LIF control*). (B) Surface expression of CD206 (*Mrc1*) was monitored by flow cytometry. An isotype-matched FITC-conjugated antibody was included to control for nonspecific staining. (C) Geometric mean fluorescence intensity of CD206 staining measured by flow cytometry was plotted for each condition. (D) Expression levels of inducible NO synthase (iNOS) and arginase-1 (ARG1) were monitored by western blotting. Total amounts of β-actin were used as a loading control. (E) Nitrite (NO_2^-) levels in culture supernatants were quantified using the Griess reaction as an indirect measurement of NO production. (F) Arginase enzymatic activity was measured in BMDM cultures according to the indicated treatment regiments. Where applicable, data are plotted as means (SD) calculated from 3 independent biological replicates. Differences were considered significant when $^{***}P < 0.001$. $^{**}P < 0.01$, and $^{*}P < 0.05$. *ns*, not significant.

Even though we did not find an increased expression of *Msr1* in our data sets, we detected the upregulation of other transcripts associated with increased processing and esterification of internalized lipids (*i.e. Lipg*, *Soat2*)[64] which could lead to the observed higher lipid accumulation in LIF-treated macrophages.

Lipid mediators are known to either promote (*i.e.* classic eicosanoids, prostaglandins, and leukotrienes) or resolve (*i.e.* resolvins, protectins, and maresins) inflammation.[65] Our data indicate that the expression of leukotriene (*Ltb4r1*), cysteinyl leukotriene (*Cysltr1*) and prostaglandin (*Ptger3*, *Ptger4*) receptors increases upon LIF stimulation which could have a profound effect in macrophage responses. For instance, macrophage LTB4R1 plays a key role in the promotion of inflammatory insulin resistance in obese mice[66] while cysteinyl leukotrienes have been associated with increased macrophage MMP9 release, and reactive oxygen species (ROS), CCL-2 and IL-8 production.[67] However, LIF-driven expression of lipid receptors could also favor macrophage tissue repair capacity, as evidenced by the regenerative role of $CD206^+$ and PTGER4-expressing intestinal macrophages in a model of colitis.[68] Collectively, our data support the notion that LIF induces transcriptional programs that affect the lipid-loading capacity and lipid mediator responsiveness of macrophages.

LIF is an immunomodulatory cytokine reported to promote or inhibit inflammatory processes.[3] Increased LIF levels in serum have been detected during acute and chronic inflammatory infections, including COVID-19,[69] and have been directly correlated with disease severity, as reported during meningococcemia.[70] *In silico* analysis of our RNA-seq data sets identified a functional subset of transcripts associated with macrophage classical activation. However, after assessing the effect of LIF priming on the response of BMDM to a combination of M1-polarizing stimuli

(LPS and IFNγ), we found no major differences in NO production or M1 marker expression. This could be in part attributed to the modest yet statistically significant transcriptional upregulation of some of the transcripts that might be insufficient to potentiate the response to M1-polarizing stimuli. Furthermore, some of the transcripts in this signature, such as *Acod1* have been reported to either promote or inhibit M1 polarization.[71,72] Further characterization of the molecular mechanisms of LIF-dependent modulation of macrophage phenotypes and functions will shed light on this matter.

Numerous reports indicate that LIF skews macrophage responses toward immunosuppressive or M2-like phenotypes.[3,31–34] This could be partially explained, through STAT3 activation, which has extensively been associated with anti-inflammatory responses in macrophages,[50] while STAT3 deficiency in BMDM has been linked to an M1-like phenotype.[73] In line with these observations, we provide evidence that LIF-primed BMDM are sensitized to IL-4 stimulation which might be in part due to STAT3-dependent upregulation of IL-4Ra, a key player in M2 polarization.[30] However, we cannot rule out the possibility that LIF upregulation of M2 responses could be multifactorial. In support of this notion, we found that LIF induces the expression of *Kdm6b*, a transcript encoding for JMJD3, a histone demethylase known to promote M2 differentiation in response to helminth infection via IRF4 epigenetic upregulation.[74] Additionally, LIF failure to enhance M1 macrophage polarization could also be due to a posttranscriptional regulatory mechanism. For instance, microRNAs are recognized as important regulators of macrophage differentiation.[75] Among them, mir-93 is known to promote M2 macrophage polarization[76] by inhibiting IRG1-dependent itaconate production. Of note, expression of mir-93 was reported to be highly upregulated upon LIF stimulation.[77] As highlighted by a recent study using a 3D in vitro model, IL-4/IL-13 M2 polarized macrophages promote wound healing by inducing myofibroblast differentiation.[78] Hence, by potentiating IL-4 driven M2 polarization and expression of tissue repair–associated transcripts (e.g. *Fn* and *Ptger4*), LIF could be a pivotal regulator of this process, as supported by our study along with previous reports.[14–16] Conversely, depending on the polarizing stimulus, M2 macrophages can be grouped in 4 different categories. Accordingly, M2a (induced by IL-4 and IL-13 stimulation), M2b (LPS and immune complexes), M2c (IL-10), and M2d (TLR ligands and A2 adenosine receptor agonists) macrophages have been characterized.[79] It would be worth investigating whether LIF-promoting effect on IL-4-driven macrophage polarization extends to other M2 subtypes.

In all, our characterization of the macrophage transcriptomic response to LIF has uncovered transcriptional programs associated with lipid metabolism and cell activation that appear to contribute to enhanced lipid-loading capacity and IL-4-polarizing sensitivity. Future investigation using a combination of in vivo, ex vivo, and in vitro functional and mechanistic studies will continue to shed light on the impact of LIF on homeostasis and disease (e.g. cancer, metabolic disorder, and infections) which could inform novel therapeutic strategies via reprogramming of macrophage phenotypes.

Acknowledgments

We wish to thank Jessie Tremblay at the INRS-CAFSB for assistance with FACS and confocal microscopy data acquisition and Patrick Gendron, Director of Information Technology and Bioinformatics at the Institut de recherche en immunologie et en cancérologie (IRIC) de l'Université Montreal for bioinformatical analyses.

Author contributions

V.C., L.-P.L., S.C., and M.J. conceived the study. V.C., L.-P.L., A.L., S.C., and M.J. designed experiments. V.C., L.-P.L., and A.L. performed experiments. V.C., L.-P.L., A.L., T.E.G., and M.J. analyzed data. T.E.G. and T.A. contributed with new technologies, reagents, and analysis tools. V.C., L.-P.L., and M.J. wrote the manuscript. All authors reviewed and edited the manuscript.

Supplementary material

Supplementary materials are available at *Journal of Leukocyte Biology* online.

Funding

This work was supported by a Natural Sciences and Engineering Research Council of Canada (NSERC) Discovery Grant to M.J. (RGPIN-2019-06671). M.J. holds a salary award *Chercheur boursier Senior* from Fonds de Recherche du Québec en santé (FRQS). A.L. was supported by a doctoral scholarship from the Pasteur Network. The funders had no role in the study design, data collection and analysis, decision to publish, or preparation of the manuscript.

Conflict of interest statement. None declared.

Data availability

The data sets generated for this study are available upon request to the corresponding authors.

References

1. Rose-John S. Interleukin-6 family cytokines. *Cold Spring Harb Perspect Biol*. 2018:10(2):a028415. https://doi.org/10.1101/cshperspect.a028415
2. Nicola NA, Babon JJ. Leukemia inhibitory factor (LIF). *Cytokine Growth Factor Rev*. 2015:26(5):533–544. https://doi.org/10.1016/j.cytogfr.2015.07.001
3. Wang J, Chang CY, Yang X, Zhou F, Liu J, Feng Z, Hu W. Leukemia inhibitory factor, a double-edged sword with therapeutic implications in human diseases. *Mol Ther*. 2023:31(2):331–343. https://doi.org/10.1016/j.ymthe.2022.12.016
4. Aghajanova L. Leukemia inhibitory factor and human embryo implantation. *Ann N Y Acad Sci*. 2004:1034(1):176–183. https://doi.org/10.1196/annals.1335.020
5. Cao W, Yang Y, Wang Z, Liu A, Fang L, Wu F, Hong J, Shi Y, Leung S, Dong C, *et al*. Leukemia inhibitory factor inhibits T helper 17 cell differentiation and confers treatment effects of neural progenitor cell therapy in autoimmune disease. *Immunity*. 2011:35(2):273–284. https://doi.org/10.1016/j.immuni.2011.06.011
6. He Z, Li JJ, Zhen CH, Feng LY, Ding XY. Effect of leukemia inhibitory factor on embryonic stem cell differentiation: implications for supporting neuronal differentiation. *Acta Pharmacol Sin*. 2006:27(1):80–90. https://doi.org/10.1111/j.1745-7254.2006.00254.x
7. Li X, Yang Q, Yu H, Wu L, Zhao Y, Zhang C, Yue X, Liu Z, Wu H, Haffty BG, *et al*. LIF promotes tumorigenesis and metastasis of breast cancer through the AKT-mTOR pathway. *Oncotarget*. 2014:5(3):788–801. https://doi.org/10.18632/oncotarget.1772
8. Rolfe BE, Stamatiou S, World CJ, Brown L, Thomas AC, Bingley JA, Worth NF, Campbell JH. Leukaemia inhibitory factor retards the progression of atherosclerosis. *Cardiovasc Res*. 2003:58(1):222–230. https://doi.org/10.1016/S0008-6363(02)00832-5

9. Langlais D, Couture C, Balsalobre A, Drouin J. Regulatory network analyses reveal genome-wide potentiation of LIF signaling by glucocorticoids and define an innate cell defense response. *PLoS Genet*. 2008:4(10):e1000224. https://doi.org/10.1371/journal.pgen.1000224
10. Langlais D, Couture C, Balsalobre A, Drouin J. The STAT3/GR interaction code: predictive value of direct/indirect DNA recruitment for transcription outcome. *Mol Cell*. 2012:47(1):38–49. https://doi.org/10.1016/j.molcel.2012.04.021
11. Salleh N, Giribabu N. Leukemia inhibitory factor: roles in embryo implantation and in nonhormonal contraception. *ScientificWorldJournal*. 2014:2014:201514. https://doi.org/10.1155/2014/201514
12. Suman P, Gupta SK. STAT3 and ERK1/2 cross-talk in leukaemia inhibitory factor mediated trophoblastic JEG-3 cell invasion and expression of mucin 1 and fos. *Am J Reprod Immunol*. 2014:72(1):65–74. https://doi.org/10.1111/aji.12248
13. Suman P, Shembekar N, Gupta SK. Leukemia inhibitory factor increases the invasiveness of trophoblastic cells through integrated increase in the expression of adhesion molecules and pappalysin 1 with a concomitant decrease in the expression of tissue inhibitor of matrix metalloproteinases. *Fertil Steril*. 2013:99(2):533–542. https://doi.org/10.1016/j.fertnstert.2012.10.004
14. Foronjy RF, Dabo AJ, Cummins N, Geraghty P. Leukemia inhibitory factor protects the lung during respiratory syncytial viral infection. *BMC Immunol*. 2014:15(1):41. https://doi.org/10.1186/s12865-014-0041-4
15. Na E, Allen E, Baird LA, Odom CV, Korkmaz FT, Shenoy AT, Matschulat AM, Jones MR, Kotton DN, Mizgerd JP, *et al*. Epithelial lif signaling limits apoptosis and lung injury during bacterial pneumonia. *Am J Physiol Lung Cell Mol Physiol*. 2022:322(4):L550–L563. https://doi.org/10.1152/ajplung.00325.2021
16. Quinton LJ, Mizgerd JP, Hilliard KL, Jones MR, Kwon CY, Allen E. Leukemia inhibitory factor signaling is required for lung protection during pneumonia. *J Immunol*. 2012:188(12):6300–6308. https://doi.org/10.4049/jimmunol.1200256
17. Tjernlund A, Walther-Jallow L, Behbahani H, Screpanti V, Nowak P, Grandien A, Andersson J, Patterson BK. Leukemia inhibitor factor (LIF) inhibits HIV-1 replication via restriction of STAT 3 activation. *AIDS Res Hum Retroviruses*. 2007:23(3):398–406. https://doi.org/10.1089/aid.2006.0100
18. Patterson BK, Behbahani H, Kabat WJ, Sullivan Y, O'Gorman MR, Landay A, Flener Z, Khan N, Yogev R, Andersson J. Leukemia inhibitory factor inhibits HIV-1 replication and is upregulated in placentae from nontransmitting women. *J Clin Invest*. 2001:107(3):287–294. https://doi.org/10.1172/JCI11481
19. Gao W, Thompson L, Zhou Q, Putheti P, Fahmy TM, Strom TB, Metcalfe SM. Treg versus Th17 lymphocyte lineages are cross-regulated by LIF versus Il-6. *Cell Cycle*. 2009:8(9):1444–1450. https://doi.org/10.4161/cc.8.9.8348
20. Janssens K, Van den Haute C, Baekelandt V, Lucas S, van Horssen J, Somers V, Van Wijmeersch B, Stinissen P, Hendriks JJ, Slaets H, *et al*. Leukemia inhibitory factor tips the immune balance towards regulatory T cells in multiple sclerosis. *Brain Behav Immun*. 2015:45:180–188. https://doi.org/10.1016/j.bbi.2014.11.010
21. Zhang YS, Xin DE, Wang Z, Song X, Sun Y, Zou QC, Yue J, Zhang C, Zhang JM, Liu Z, *et al*. STAT4 activation by leukemia inhibitory factor confers a therapeutic effect on intestinal inflammation. *EMBO J*. 2019:38(6):e99595. https://doi.org/10.15252/embj.201899595
22. Sesti-Costa R, Cervantes-Barragan L, Swiecki MK, Fachi JL, Cella M, Gilfillan S, Silva JS, Colonna M. Leukemia inhibitory factor inhibits plasmacytoid dendritic cell function and development. *J Immunol*. 2020:204(8):2257–2268. https://doi.org/10.4049/jimmunol.1900604
23. Yaftiyan A, Eskandarian M, Jahangiri AH, Kazemi Sefat NA, Moazzeni SM. Leukemia inhibitory factor (LIF) modulates the development of dendritic cells in a dual manner. *Immunopharmacol Immunotoxicol*. 2019:41(3):455–462. https://doi.org/10.1080/08923973.2019.1619761
24. Zheng X, Knight DA, Zhou D, Weir T, Peacock C, Schellenberg RR, Bai TR. Leukemia inhibitory factor is synthesized and released by human eosinophils and modulates activation state and chemotaxis. *J Allergy Clin Immunol*. 1999:104(1):136–144. https://doi.org/10.1016/S0091-6749(99)70125-9
25. Hilton DJ, Nicola NA, Metcalf D. Distribution and comparison of receptors for leukemia inhibitory factor on murine hemopoietic and hepatic cells. *J Cell Physiol*. 1991:146(2):207–215. https://doi.org/10.1002/jcp.1041460204
26. Naito M. Macrophage differentiation and function in health and disease. *Pathol Int*. 2008:58(3):143–155. https://doi.org/10.1111/j.1440-1827.2007.02203.x
27. Locati M, Curtale G, Mantovani A. Diversity, mechanisms, and significance of macrophage plasticity. *Annu Rev Pathol*. 2020:15(1):123–147. https://doi.org/10.1146/annurev-pathmechdis-012418-012718
28. Qiao Y, Giannopoulou EG, Chan CH, Park SH, Gong S, Chen J, Hu X, Elemento O, Ivashkiv LB. Synergistic activation of inflammatory cytokine genes by interferon-gamma-induced chromatin remodeling and toll-like receptor signaling. *Immunity*. 2013:39(3):454–469. https://doi.org/10.1016/j.immuni.2013.08.009
29. Bose D, Banerjee S, Chatterjee N, Das S, Saha M, Saha KD. Inhibition of TGF-beta induced lipid droplets switches M2 macrophages to M1 phenotype. *Toxicol In Vitro*. 2019:58:207–214. https://doi.org/10.1016/j.tiv.2019.03.037
30. Martinez FO, Helming L, Gordon S. Alternative activation of macrophages: an immunologic functional perspective. *Annu Rev Immunol*. 2009:27(1):451–483. https://doi.org/10.1146/annurev.immunol.021908.132532
31. Duluc D, Delneste Y, Tan F, Moles MP, Grimaud L, Lenoir J, Preisser L, Anegon I, Catala L, Ifrah N, *et al*. Tumor-associated leukemia inhibitory factor and Il-6 skew monocyte differentiation into tumor-associated macrophage-like cells. *Blood*. 2007:110(13):4319–4330. https://doi.org/10.1182/blood-2007-02-072587
32. Yu S, Li Q, Wang Y, Cui Y, Yu Y, Li W, Liu F, Liu T. Tumor-derived LIF promotes chemoresistance via activating tumor-associated macrophages in gastric cancers. *Exp Cell Res*. 2021:406(1):112734. https://doi.org/10.1016/j.yexcr.2021.112734
33. Dallagi A, Girouard J, Hamelin-Morrissette J, Dadzie R, Laurent L, Vaillancourt C, Lafond J, Carrier C, Reyes-Moreno C. The activating effect of IFN-gamma on monocytes/macrophages is regulated by the LIF-trophoblast-Il-10 axis via STAT1 inhibition and STAT3 activation. *Cell Mol Immunol*. 2015:12(3):326–341. https://doi.org/10.1038/cmi.2014.50
34. Hamelin-Morrissette J, Dallagi A, Girouard J, Ravelojaona M, Oufqir Y, Vaillancourt C, Van Themsche C, Carrier C, Reyes-Moreno C. Leukemia inhibitory factor regulates the activation of inflammatory signals in macrophages and trophoblast cells. *Mol Immunol*. 2020:120:32–42. https://doi.org/10.1016/j.molimm.2020.01.021
35. Chaparro V, Leroux LP, Masvidal L, Lorent J, Graber TE, Zimmermann A, Arango Duque G, Descoteaux A, Alain T, Larsson O, *et al*. Translational profiling of macrophages infected with *Leishmania donovani* identifies mTOR- and eIF4A-sensitive

immune-related transcripts. *PLoS Pathog*. 2020:16(6):e1008291. https://doi.org/10.1371/journal.ppat.1008291
36. Taylor S, Wakem M, Dijkman G, Alsarraj M, Nguyen M. A practical approach to RT-qPCR-publishing data that conform to the miqe guidelines. *Methods*. 2010:50(4):S1–S5. https://doi.org/10.1016/j.ymeth.2010.01.005
37. Bolger AM, Lohse M, Usadel B. Trimmomatic: a flexible trimmer for Illumina sequence data. *Bioinformatics*. 2014:30(15):2114–2120. https://doi.org/10.1093/bioinformatics/btu170
38. Dobin A, Davis CA, Schlesinger F, Drenkow J, Zaleski C, Jha S, Batut P, Chaisson M, Gingeras TR. Star: ultrafast universal RNA-seq aligner. *Bioinformatics*. 2013:29(1):15–21. https://doi.org/10.1093/bioinformatics/bts635
39. Li B, Dewey CN. RSEM: accurate transcript quantification from RNA-seq data with or without a reference genome. *BMC Bioinformatics*. 2011:12(1):323. https://doi.org/10.1186/1471-2105-12-323
40. Love MI, Huber W, Anders S. Moderated estimation of fold change and dispersion for RNA-seq data with DESeq2. *Genome Biol*. 2014:15(12):550. https://doi.org/10.1186/s13059-014-0550-8
41. Pasquin S, Laplante V, Kouadri S, Milasan A, Mayer G, Tormo AJ, Savin V, Sharma M, Martel C, Gauchat JF. Cardiotrophin-like cytokine increases macrophage-foam cell transition. *J Immunol*. 2018:201(8):2462–2471. https://doi.org/10.4049/jimmunol.1800733
42. Rabhi S, Rabhi I, Trentin B, Piquemal D, Regnault B, Goyard S, Lang T, Descoteaux A, Enninga J, Guizani-Tabbane L. Lipid droplet formation, their localization and dynamics during *Leishmania major* macrophage infection. *PLoS One*. 2016:11(2):e0148640. https://doi.org/10.1371/journal.pone.0148640
43. Leroux LP, Lorent J, Graber TE, Chaparro V, Masvidal L, Aguirre M, Fonseca BD, van Kempen LC, Alain T, Larsson O, *et al.* The protozoan parasite *Toxoplasma gondii* selectively reprograms the host cell translatome. *Infect Immun*. 2018:86(9):e00244-18. https://doi.org/10.1128/IAI.00244-18
44. William M, Leroux LP, Chaparro V, Lorent J, Graber TE, M'Boutchou MN, Charpentier T, Fabie A, Dozois CM, Stager S, *et al.* EIF4E-binding proteins 1 and 2 limit macrophage anti-inflammatory responses through translational repression of Il-10 and cyclooxygenase-2. *J Immunol*. 2018:200(12):4102–4116. https://doi.org/10.4049/jimmunol.1701670
45. Jaramillo M, Gomez MA, Larsson O, Shio MT, Topisirovic I, Contreras I, Luxenburg R, Rosenfeld A, Colina R, McMaster RW, *et al. Leishmania* repression of host translation through mTOR cleavage is required for parasite survival and infection. *Cell Host Microbe*. 2011:9(4):331–341. https://doi.org/10.1016/j.chom.2011.03.008
46. Leroux LP, Nasr M, Valanparambil R, Tam M, Rosa BA, Siciliani E, Hill DE, Zarlenga DS, Jaramillo M, Weinstock JV, *et al.* Analysis of the *Trichuris suis* excretory/secretory proteins as a function of life cycle stage and their immunomodulatory properties. *Sci Rep*. 2018:8(1):15921. https://doi.org/10.1038/s41598-018-34174-4
47. Marshall MK, Doerrler W, Feingold KR, Grunfeld C. Leukemia inhibitory factor induces changes in lipid metabolism in cultured adipocytes. *Endocrinology*. 1994:135(1):141–147. https://doi.org/10.1210/endo.135.1.8013346
48. Yang X, Wang J, Chang CY, Zhou F, Liu J, Xu H, Ibrahim M, Gomez M, Guo GL, Liu H, *et al.* Leukemia inhibitory factor suppresses hepatic de novo lipogenesis and induces cachexia in mice. *Nat Commun*. 2024:15(1):627. https://doi.org/10.1038/s41467-024-44924-w
49. Greenspan P, Yu H, Mao F, Gutman RL. Cholesterol deposition in macrophages: foam cell formation mediated by cholesterol-enriched oxidized low density lipoprotein. *J Lipid Res*. 1997:38(1):101–109. https://doi.org/10.1016/S0022-2275(20)37279-5
50. Xia T, Zhang M, Lei W, Yang R, Fu S, Fan Z, Yang Y, Zhang T. Advances in the role of STAT3 in macrophage polarization. *Front Immunol*. 2023:14:1160719. https://doi.org/10.3389/fimmu.2023.1160719
51. Hutchins AP, Poulain S, Miranda-Saavedra D. Genome-wide analysis of STAT3 binding in vivo predicts effectors of the anti-inflammatory response in macrophages. *Blood*. 2012:119(13):e110–e119. https://doi.org/10.1182/blood-2011-09-381483
52. Carl VS, Gautam JK, Comeau LD, Smith MFJr. Role of endogenous Il-10 in LPS-induced STAT3 activation and Il-1 receptor antagonist gene expression. *J Leukoc Biol*. 2004:76(3):735–742. https://doi.org/10.1189/jlb.1003526
53. Alhayyani S, McLeod L, West AC, Balic JJ, Hodges C, Yu L, Smith JA, Prodanovic Z, Bozinovski S, Kumar B, *et al.* Oncogenic dependency on STAT3 serine phosphorylation in KRAS mutant lung cancer. *Oncogene*. 2022:41(6):809–823. https://doi.org/10.1038/s41388-021-02134-4
54. Balic JJ, Garama DJ, Saad MI, Yu L, West AC, West AJ, Livis T, Bhathal PS, Gough DJ, Jenkins BJ. Serine-phosphorylated STAT3 promotes tumorigenesis via modulation of RNA polymerase transcriptional activity. *Cancer Res*. 2019:79(20):5272–5287. https://doi.org/10.1158/0008-5472.CAN-19-0974
55. Balic JJ, Saad MI, Dawson R, West AJ, McLeod L, West AC, D'Costa K, Deswaerte V, Dev A, Sievert W, *et al.* Constitutive STAT3 serine phosphorylation promotes helicobacter-mediated gastric disease. *Am J Pathol*. 2020:190(6):1256–1270. https://doi.org/10.1016/j.ajpath.2020.01.021
56. Dimri S, Malhotra R, Shet T, Mokal S, Gupta S, De A. Noncanonical pS727 post translational modification dictates major STAT3 activation and downstream functions in breast cancer. *Exp Cell Res*. 2020:396(2):112313. https://doi.org/10.1016/j.yexcr.2020.112313
57. Lang R, Patel D, Morris JJ, Rutschman RL, Murray PJ. Shaping gene expression in activated and resting primary macrophages by Il-10. *J Immunol*. 2002:169(5):2253–2263. https://doi.org/10.4049/jimmunol.169.5.2253
58. Schust J, Sperl B, Hollis A, Mayer TU, Berg T. Stattic: a small-molecule inhibitor of STAT3 activation and dimerization. *Chem Biol*. 2006:13(11):1235–1242. https://doi.org/10.1016/j.chembiol.2006.09.018
59. Aubert J, Dessolin S, Belmonte N, Li M, McKenzie FR, Staccini L, Villageois P, Barhanin B, Vernallis A, Smith AG, *et al.* Leukemia inhibitory factor and its receptor promote adipocyte differentiation via the mitogen-activated protein kinase cascade. *J Biol Chem*. 1999:274(35):24965–24972. https://doi.org/10.1074/jbc.274.35.24965
60. Belmonte N, Phillips BW, Massiera F, Villageois P, Wdziekonski B, Saint-Marc P, Nichols J, Aubert J, Saeki K, Yuo A, *et al.* Activation of extracellular signal-regulated kinases and CREB/ATF-1 mediate the expression of CCAAT/enhancer binding proteins beta and -delta in preadipocytes. *Mol Endocrinol*. 2001:15(11):2037–2049. https://doi.org/10.1210/mend.15.11.0721
61. Hogan JC, Stephens JM. Effects of leukemia inhibitory factor on 3T3-L1 adipocytes. *J Endocrinol*. 2005:185(3):485–496. https://doi.org/10.1677/joe.1.05980
62. Gimble JM, Wanker F, Wang CS, Bass H, Wu X, Kelly K, Yancopoulos GD, Hill MR. Regulation of bone marrow stromal cell differentiation by cytokines whose receptors share the GP130 protein. *J Cell Biochem*. 1994:54(1):122–133. https://doi.org/10.1002/jcb.240540113

63. Moran CS, Campbell JH, Campbell GR. Human leukemia inhibitory factor upregulates LDL receptors on liver cells and decreases serum cholesterol in the cholesterol-fed rabbit. *Arterioscler Thromb Vasc Biol*. 1997:17(7):1267–1273. https://doi.org/10.1161/01.ATV.17.7.1267
64. Levitan I, Volkov S, Subbaiah PV. Oxidized LDL: diversity, patterns of recognition, and pathophysiology. *Antioxid Redox Signal*. 2010:13(1):39–75. https://doi.org/10.1089/ars.2009.2733
65. Serhan CN, Chiang N, Dalli J, Levy BD. Lipid mediators in the resolution of inflammation. *Cold Spring Harb Perspect Biol*. 2014:7(2):a016311. https://doi.org/10.1101/cshperspect.a016311
66. Li P, Oh DY, Bandyopadhyay G, Lagakos WS, Talukdar S, Osborn O, Johnson A, Chung H, Maris M, Ofrecio JM, *et al*. LTB4 promotes insulin resistance in obese mice by acting on macrophages, hepatocytes and myocytes. *Nat Med*. 2015:21(3):239–247. https://doi.org/10.1038/nm.3800
67. Theron AJ, Steel HC, Tintinger GR, Gravett CM, Anderson R, Feldman C. Cysteinyl leukotriene receptor-1 antagonists as modulators of innate immune cell function. *J Immunol Res*. 2014:2014:608930. https://doi.org/10.1155/2014/608930
68. Na YR, Jung D, Stakenborg M, Jang H, Gu GJ, Jeong MR, Suh SY, Kim HJ, Kwon YH, Sung TS, *et al*. Prostaglandin E(2) receptor PTGER4-expressing macrophages promote intestinal epithelial barrier regeneration upon inflammation. *Gut*. 2021:70(12):2249–2260. https://doi.org/10.1136/gutjnl-2020-322146
69. Young BE, Ong SWX, Ng LFP, Anderson DE, Chia WN, Chia PY, Ang LW, Mak TM, Kalimuddin S, Chai LYA, *et al*. Viral dynamics and immune correlates of coronavirus disease 2019 (COVID-19) severity. *Clin Infect Dis*. 2021:73(9):e2932–e2942. https://doi.org/10.1093/cid/ciaa1280
70. Waring PM, Waring LJ, Metcalf D. Circulating leukemia inhibitory factor levels correlate with disease severity in meningococcemia. *J Infect Dis*. 1994:170(5):1224–1228. https://doi.org/10.1093/infdis/170.5.1224
71. Wang X, Su S, Zhu Y, Cheng X, Cheng C, Chen L, Lei A, Zhang L, Xu Y, Ye D, *et al*. Metabolic reprogramming via ACOD1 depletion enhances function of human induced pluripotent stem cell-derived CAR-macrophages in solid tumors. *Nat Commun*. 2023:14(1):5778. https://doi.org/10.1038/s41467-023-41470-9
72. Wu R, Chen F, Wang N, Tang D, Kang R. ACOD1 in immunometabolism and disease. *Cell Mol Immunol*. 2020:17(8):822–833. https://doi.org/10.1038/s41423-020-0489-5
73. Farmand S, Sender V, Karlsson J, Merkl P, Normark S, Henriques-Normark B. STAT3 deficiency alters the macrophage activation pattern and enhances matrix metalloproteinase 9 expression during staphylococcal pneumonia. *J Immunol*. 2024:212(1):69–80. https://doi.org/10.4049/jimmunol.2300151
74. Satoh T, Takeuchi O, Vandenbon A, Yasuda K, Tanaka Y, Kumagai Y, Miyake T, Matsushita K, Okazaki T, Saitoh T, *et al*. The JMJD3-IRF4 axis regulates M2 macrophage polarization and host responses against helminth infection. *Nat Immunol*. 2010:11(10):936–944. https://doi.org/10.1038/ni.1920
75. Li H, Jiang T, Li MQ, Zheng XL, Zhao GJ. Transcriptional regulation of macrophages polarization by microRNAs. *Front Immunol*. 2018:9:1175. https://doi.org/10.3389/fimmu.2018.01175
76. Ganta VC, Choi MH, Kutateladze A, Fox TE, Farber CR, Annex BH. A microRNA93-interferon regulatory factor-9-immunoresponsive gene-1-itaconic acid pathway modulates M2-like macrophage polarization to revascularize ischemic muscle. *Circulation*. 2017:135(24):2403–2425. https://doi.org/10.1161/CIRCULATIONAHA.116.025490
77. Morales-Prieto DM, Schleussner E, Markert UR. Reduction in mir-141 is induced by leukemia inhibitory factor and inhibits proliferation in choriocarcinoma cell line JEG-3. *Am J Reprod Immunol*. 2011:66(Suppl 1):57–62. https://doi.org/10.1111/j.1600-0897.2011.01037.x
78. Sapudom J, Karaman S, Mohamed WKE, Garcia-Sabate A, Quartey BC, Teo JCM. 3D in vitro M2 macrophage model to mimic modulation of tissue repair. *NPJ Regen Med*. 2021:6(1):83. https://doi.org/10.1038/s41536-021-00193-5
79. Wang LX, Zhang SX, Wu HJ, Rong XL, Guo J. M2b macrophage polarization and its roles in diseases. *J Leukoc Biol*. 2019:106(2):345–358. https://doi.org/10.1002/JLB.3RU1018-378RR